Modelling the percolation-type transition in radiation damage

Kostya Trachenko
Mineral Physics, Department of Earth Sciences, University of Cambridge, Downing Street, Cambridge, CB2 3EQ, United Kingdom and Cavendish Laboratory, Madingley Road, Cambridge, CB3 0HE, United Kingdom

Martin T. Dove[a] and Ekhard Salje
Mineral Physics, Department of Earth Sciences, University of Cambridge, Downing Street, Cambridge, CB2 3EQ, United Kingdom

(Received 5 October 1999; accepted for publication 6 March 2000)

Following the concept of percolation-type transition in zircon under radiation damage suggested previously, the general simulation model of irradiated material is proposed. The model naturally gives rise to swelling of the undamaged crystalline part of irradiated material. X-ray scattering profiles are calculated and show broadening that increases with radiation damage, in good agreement with published experimental x-ray diffraction data on zircon. The effect of percolation on material bulk properties is studied. © *2000 American Institute of Physics.* [S0021-8979(00)08711-9]

I. INTRODUCTION

The study of radiation damage in zircon has recently received a lot of attention. During alpha-decay-induced irradiation damage in zircon an energetic recoil nucleus produces a displacement cascade consisting of about 1000 atoms and an alpha particle produces several hundred isolated atomic displacements. The important question concerns the nature of the amorphization process at the local level, whether it happens directly within the displacement cascade or as a result of the overlap of individual damaged regions. It was suggested that in zircon,[1,2] unlike in other complex silicate structures, the alpha-decay-induced amorphization process is consistent with models based on the multiple overlap of displacement cascades.[3] This indicated that amorphization in zircon occurs as a result of the collapse of the crystalline structure after the local concentration of defects reaches some critical point, rather than directly in the displacement cascade. However, more recent experimental data on zircon[4] indicated that amorphization is consistent with the single overlap model.[3]

More recent work[5] has concentrated on the transition from the crystalline to amorphous state on a macroscopic length scale and the main question asked was whether this transition can be treated as a ''driven'' phase transition with critical dose at the transition point, as was considered earlier. In Ref. 5 it was argued that a careful distinction should be made between the damage process on the local and macroscopic level. While on the local level the collapse of the crystalline structure into an amorphous state is a driven phase transition with a critical dose, no experimental evidence exists to support this view on the macroscopic scale. Instead, a percolation-type transition was proposed in Ref. 5 which introduces two critical doses which correspond to percolation points.

The percolation model, with its two percolation points, has the following effects on the structure of the damaged material. At the first percolation point amorphous regions, which are separated from all others in the crystalline matrix at lower dose, form the percolating cluster which connects the top and the bottom of the sample. At the second percolation point crystalline islands, which were interconnected at lower dose, cease to form a percolating cluster and become disconnected in the amorphous matrix. The percolation-type transition model describes amorphization as a gradual process, with an order parameter related to the periodicity of the crystalline structure.[5]

The purpose of the present work is to simulate the effects related to volume swelling and diffuse scattering arising from the percolation-type transition in irradiated material, and to investigate the effect of percolation on the bulk properties of irradiated material. In order to do this, we propose a general model to simulate the irradiated material and percolation. This model allows us to visualize the changes that occur in the structure under irradiation. We find that the scattering profiles calculated from this model are in good agreement with recent experimental data on irradiated zircon. In addition, we find that our model provides the mechanism for swelling of the undamaged crystalline regions caused by the stress imposed by adjacent amorphous regions in the tangent direction.

II. THE MODEL OF IRRADIATED MATERIAL: PERCOLATION

Central to the development of our computer model of irradiated material is the assumption that the radiation damage leads to the formation of a certain number of regions which are amorphous. We set aside the issue of the details of the mechanism involved in forming the amorphous regions, for our main interest is to study the irradiation damage on a macroscopic level. We represent the whole sample by a cubic primitive lattice with each point representing a region of

[a]Author to whom correspondence should be addressed; electronic mail: martin@esc.cam.ac.uk

the crystal (i.e., many unit cells) which can be either amorphous or crystalline. Amorphous regions are introduced at random and their number N_a is set according to a given concentration $f_a = N_a/N$, where N is the total number of regions, or points on our lattice. The rest of the points in the cubic lattice represent undamaged crystalline areas.

In addition to direct creation of amorphous regions, either in the displacement cascade produced by heavy recoil or by spontaneous collapse of the crystalline structure due to critical concentration of point defects, there exists an indirect mechanism which was pointed out in Ref. 5 and was seen experimentally. When a crystalline region is surrounded by amorphous ones there is a point defined by the local concentration of those amorphous regions and a size of crystalline region at which this crystalline region becomes amorphous as well. This happens when the volume of interface between a crystalline and the surrounding amorphous regions becomes large enough, relative to the size of remaining crystalline region, to cause its collapse to amorphous state.

We accounted for this indirect mechanism effect by introducing additional amorphous regions in two ways. In the *first* approach, which we call the ''one-step approach,'' each crystalline region that happened to be surrounded by two amorphous ones introduced originally was also made amorphous, and no further amorphous regions were introduced. In the *second* approach, which we call the ''multi-step approach,'' every additional amorphous region introduced was also allowed to convert a neighboring crystalline region into an amorphous region as in the one-step approach, and the process was repeated until there were no crystalline regions left surrounded by two amorphous neighbors. On a microscopic level, the issue of which approach better reflects the associated physical processes is related to the question of whether the amorphous region created by the collapse of crystalline structure as a result of the presence of adjacent amorphous regions can impose the same effect on the crystalline regions left around it as the original amorphous regions produced by irradiation.

To illustrate the effect of the choice of either approach on a macroscopic level, we denote p as the final concentration of amorphous areas, including additional ones introduced through the above mechanism. We introduced amorphous regions at random in our cubic lattice according to a number of initial concentrations f_a (defined earlier). Additional amorphous regions were introduced according to either one-step or multi-step approach and counted, giving a final concentration of amorphous areas p. Using the algorithms described above, we constructed the dependence $p = p(f_a)$ for single-step and multi-step approaches, which is shown on Fig. 1. Since in the multi-step approach every newly introduced amorphous region participates in the appearance of additional neighboring amorphous regions, this approach resulted in a steeper dependence of p on f_a than the single-step approach. This effect can be seen to be particularly significant at the intermediate values of f_a. On the other hand, we studied the macroscopic expansion, unit cell expansion and scattering profiles (see sections below) of the structures derived in both approaches and found no difference between the results of the two methods. As might have been expected, these macroscopic features depend on the value of the final concentration of amorphous areas in the structure only and do not depend on whether the one-step or the multi-step approach is used to arrive at that value of concentration.

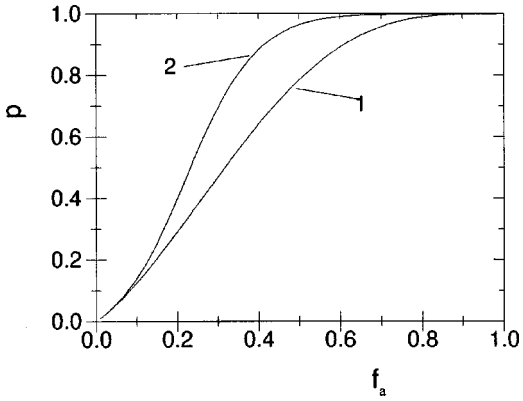

FIG. 1. Final concentration of amorphous points p vs f_a derived in one-step approach (1) and multi-step approach (2).

To simulate the first and second percolation points, which were defined earlier, we constructed a cubic lattice containing $100\times100\times100$ points, with each point representing either a crystalline or an amorphous region. When increasing the portion of ''amorphous'' points we checked at each value of f_a whether the cluster formed by amorphous points starts connecting the top and the bottom of our simulation box.[6] This value defines the first percolation point $f_a = f1$. Similarly, the second percolation point $f_a = f2$ is defined by the value of f_a at which the cluster formed by ''crystalline'' points stops connecting the top and the bottom of our simulation box.

We give the values of $f1$, $f2$ and corresponding final concentrations p for each of the two approaches described above, together with the case when no additional amorphous regions were introduced, which we call the ''direct'' approach, in Table I. We note that for the direct case the calculated value of $f1$ is in good agreement with the known value of the percolation point for a cubic lattice $f1 = 0.312$.[6] It is interesting to see that, according to Table I, the introduction of new additional amorphous points using either of the methods significantly speeds up the percolation in that a much lower value of the final concentration p is needed to reach the first percolation point, such that $p(f1)$ has values 0.185 and 0.172 in the two approaches compared with $p(f1) = 0.316$ when no additional amorphous regions are introduced. The introduction of additional amorphous points breaks the randomness of distribution of amorphous points throughout the sample and promotes connectivity of amor-

TABLE I. Values of f_a at the first and second percolation points and corresponding final concentrations.

	$f1$	$p(f1)$	$f2$	$p(f2)$
direct approach	0.316	0.316	0.689	0.689
one-step approach	0.138	0.185	0.476	0.753
multi-step approach	0.116	0.172	0.341	0.785

phous clusters and percolation. The same mechanism explains the larger value of the second percolation point $p(f2)$ when additional amorphous points are introduced, as compared with the direct approach. We note that in the direct approach, with random distribution of amorphous and crystalline points, $p(f1)+p(f2)=1$ (within the computation error), while this relation does not hold in one-step and multi-step approaches (Table I).

It should be noted that the one-step and multi-step approaches yield almost the same value of final concentrations p at the first and second percolation points (Table I). This indicates that the final structures derived using those two approaches differ mostly by the distribution of amorphous and crystalline areas in them, and not by the numbers of those areas which makes the choice of either approach insignificant. Below we use the one-step approach in studying percolation as well as other macroscopic features.

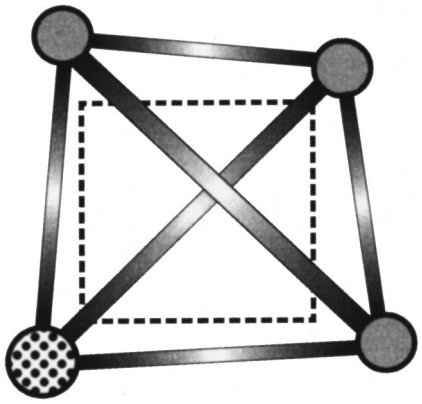

FIG. 2. Schematic representation of modeling the distortion in the lattice due to introduction of amorphous areas. Shaded circles represent crystalline areas and selected circle represents an amorphous area.

III. VOLUME SWELLING

One of the crucial effects of introducing the amorphous areas in the material due to irradiation is the swelling of the amorphous area relative to the pure crystal. This distorts the rest of the crystalline structure by imposing stress on adjacent crystalline regions. One straightforward way to obtain the resulting relaxed structure, taking into account the distortion due to swelling, is to employ the molecular dynamics simulation technique. This technique ensures that crystalline and amorphous regions move relative to each other, according to imposed local stresses, so that in the new equilibrium positions all the regions have relaxed to zero force. To simulate this relaxation we use the molecular dynamics method, treating the amorphous and crystalline regions as particles with different sizes. In this context we use the molecular dynamics as energy minimizer, rather than to study the dynamics of our system. We suppose that the distance from every amorphous point in our lattice to its next neighbor increases by a certain percentage c if that neighbor is crystalline and by $2c$ if the neighbor is amorphous. The distance between the neighbors does not change if they both happen to be crystalline. Thus the value of c serves as a measure of the swelling of the amorphous region relative to a crystalline one.

We implemented this algorithm by relaxing the structure using molecular dynamics simulation techniques with the DLPOLY package.[7] Pair Buckingham potentials were introduced between all neighbor points with parameters which yielded required values of distances between points, taking into account the swelling as defined above. The potential parameters were tuned so that a minima of potential acting between crystalline points, amorphous and crystalline points and amorphous points equal 1, $1+c$, and $1+2c$, correspondingly. We also introduced potentials acting between diagonal points which allowed the sample to keep its cubic structure during the simulation, subject to the same swelling conditions. Figure 2 schematically illustrates this procedure. It should be noted that the choice of the type of potential acting between lattice points (which represent either crystalline or amorphous regions) is insignificant, insofar as this potential is only used to relax amorphous and crystalline regions due to local swelling and distortion, i.e., to create structures with appropriate distortions and strains.

We note that the ''stress'' model built in the way outlined above is not intended to describe specific atoms or any specific system, but is designed to give strained regions according to any given distribution of crystalline and amorphous regions. It need not be specific for zircon, the system we use to compare our results with experiment, but is applicable for any system with radiation damage.

A cubic box containing $40\times40\times40$ points was chosen for the simulation. The structure was relaxed in the constant pressure and temperature ensemble, thus allowing the total volume of the structure to change. The temperature was low relatively to the interaction energy. Two slices of our structure for two values of dose which correspond to $f<f1$ and $f1<f<f2$ regimes are plotted in Fig. 3. As can be seen from the top picture in Fig. 3, the crystalline areas that are situated far from amorphous ones stay relatively undistorted if compared to those adjacent to amorphous areas. In addition to total volume swelling and translations, the distortion can be seen in the form of shearing, a point to which we return later. When the number of amorphous areas becomes dominant (bottom picture in Fig. 3), the shear distortion can be seen throughout the whole structure.

To study the effect of introducing the amorphous areas in our model, we have produced a number of relaxed configurations for various values of the f_a using the one-step approach. This allowed us to construct the dependence of total volume on dose, which is shown in Fig. 4(a). We also calculated the average distances between each of two neighboring crystalline and amorphous points for each value of the dose. The corresponding volume change of the crystalline and amorphous unit cells is shown in Fig. 4(b). We have deliberately chosen the model parameter c to be 10%, which is larger than in zircon, in order to enhance the effects of swelling to see them more clearly. Therefore the value of saturation of the total volume and unit cell swelling of zircon at high doses measured experimentally (see, for example, Refs. 1 and 2) is lower than the one obtained in our model.

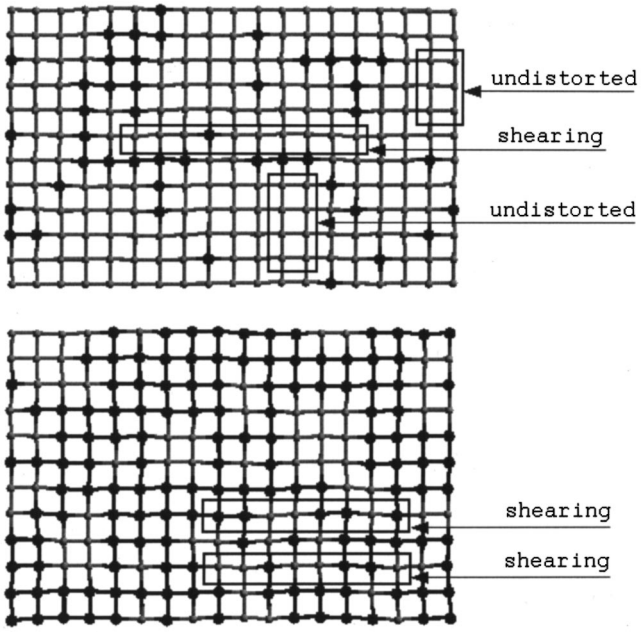

FIG. 3. Slices of relaxed configuration for $f_a=0.10$ (top) and $f_a=0.35$ (bottom). Large dark balls represent the amorphous regions and small gray balls represent the crystalline regions. Selected areas highlight relatively undistorted crystalline regions and shearing in the structure.

It is interesting to study the change in the behavior of volume swelling of the sample at the values of f_a corresponding to the first and second percolation points. At the first percolation point the amorphous cluster starts connecting the sample boundaries, but the crystalline cluster percolates until the second percolation point is reached. In this regime adding new amorphous regions is expected to lead to a gradual increase of the total volume [see Fig. 4(a)]. When the second percolation point is reached, the cluster formed by the crystalline areas no longer connects the boundaries of the sample. Disconnected crystalline regions, not being a part of one cluster, might be expected to move according to local stresses which are different throughout the sample. Increased shifting and rotating of those regions relative to each other could lead to the change in the behavior of total volume swelling. However, no apparent change in the total volume swelling can be seen in Fig. 4(a) at the second percolation point. This can be explained by noting that the volume of the crystalline unit cell increases gradually with the concentration of amorphous areas [Fig. 4(b)]. This happens even at low values of f_a and continues to be the case up to higher values $f_a > f2$. At the second percolation point the crystalline areas are already locally distorted in the form of swelling and shearing to the extent that no change in the behavior of the total volume swelling can be observed.

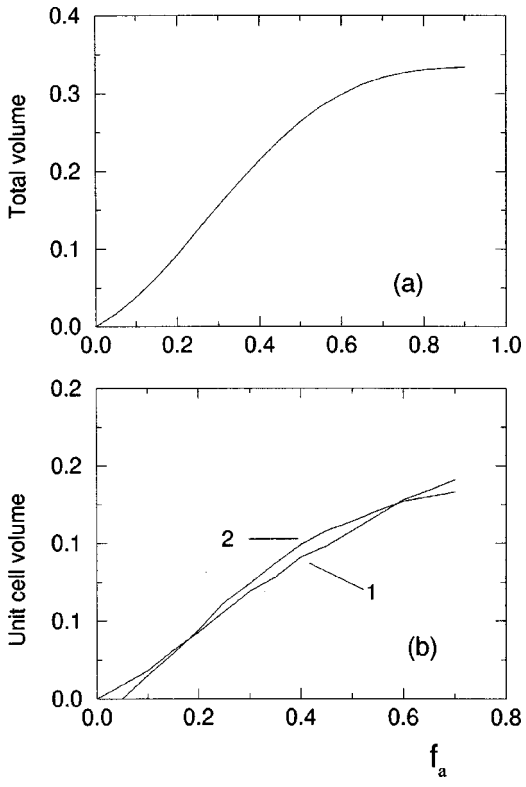

FIG. 4. Dependence of (a) total volume increase $\Delta V/V$ on f_a and (b) unit cell volume increase $\Delta V/V$ on f_a for crystalline (1) and amorphous (2) parts.

The fact that the average volume of a crystalline unit cell increases with f_a, as can be seen from Fig. 4(b), is quite interesting because the distance between two adjacent crystalline areas, or the size of the crystalline unit cell in our model, is fixed and was not set to depend on f_a. From the simulation we have the following explanation: while the stress imposed by swelling of the amorphous region on adjacent crystalline regions in the radial direction results in the total volume increase, the tangent component of the stress stretches the crystalline regions in the tangent direction, forcing them to swell. The same can be argued about swelling of the amorphous unit cell [Fig. 4(b)]. It is forced to stretch in tangent direction under the stress imposed by a newly introduced adjacent amorphous region. It is generally assumed that the measured unit-cell expansion in the irradiated material is caused by an accumulation of point defects in the crystalline regions. We conclude that in our model the swelling of crystalline parts of the structure naturally happens as a result of the tangent stress from adjacent amorphous regions.

IV. SCATTERING PROFILES

Generally, the introduction of damaged or completely amorphous areas in the material under irradiation results in the reduction of the intensity of the Bragg peak and a shift of its scattering vector and appearance of diffuse scattering in scattering profiles. Scattering profiles of irradiated material contain an important information which includes the degree of damage, swelling, distribution of areas with different degrees of damage, etc. It is therefore important to study the scattering profiles of damaged structures in our model and compare them with experimental data.

Having produced a number of configurations corresponding to various degrees of damage, we calculated scattering profiles of the form

$$I(\mathbf{Q}) = \left| \sum_j e^{i\mathbf{Q}\cdot\mathbf{R}_j} \right|^2, \tag{1}$$

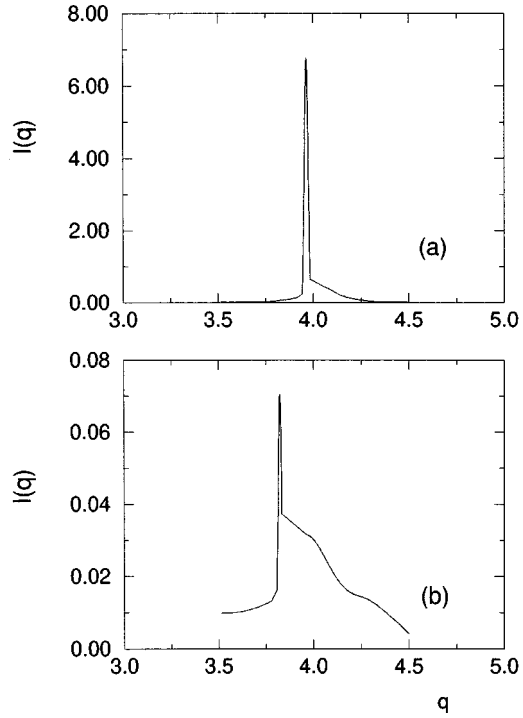

FIG. 5. Dependence of intensity $I(q)$ on q along the longitudinal direction of (440) reflection for (a) $f_a=0.20$ and (b) $f_a=0.40$.

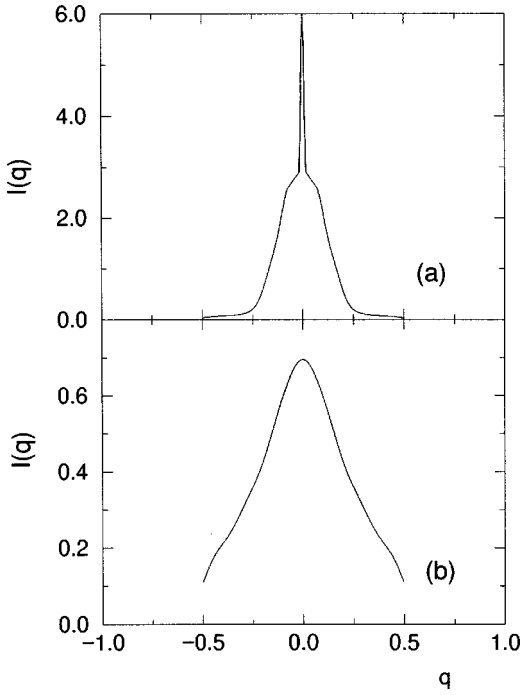

FIG. 6. Dependence of intensity $I(q)$ on q along the transverse direction of (440) reflection for (a) $f_a=0.10$ and (b) $f_a=0.20$.

where $\mathbf{Q}=\mathbf{G}+\mathbf{q}$ is the scattering vector, $\mathbf{G}$ is the closest reciprocal lattice vector, and $\mathbf{q}$ is the wave vector with respect to the Bragg reflection. In particular, the intensity distribution was calculated around the (440) and (200) reflections in order to compare with experimental x-ray diffraction data.[8] When calculating scattering profiles, only contributions from crystalline areas were taken into account. Scattering profiles were averaged over all equivalent $\mathbf{Q}$ vectors. In order to reduce statistical noise caused by the limited number of samples and their finite size, the diffuse scattering profiles were smoothed by convolution with Gaussian function. Diffuse scattering tails were convoluted separately from the Bragg peak, to preserve the height and shape of each profile.

The effects related to volume swelling can be observed in the scattering profiles calculated along the longitudinal direction of a particular reflection. The scattering profile along the longitudinal direction of (440) reflection is shown in Fig. 5 for two different values of f_a. As can be seen from this figure, increasing the dose clearly results in increased diffuse scattering tails as a result of highly inhomogeneous distortion of the structure. Due to the swelling of the unit cell, the position of the sharp Bragg peak moves from (440) to $(4-\xi,4-\xi,0)$ (ξ is a positive value less than 1 — note that the size of the reciprocal lattice vectors is fixed by the size of the sample, not by the size of the crystalline unit cell). On the other hand, the weight of the broad diffuse scattering profile remains close to (440), which is to the high side of the Bragg peak, and with significant asymmetry. This effect is consistent with the scattering profiles obtained experimentally using x-ray diffraction analysis of irradiated zircon.[5,8–10] The observed asymmetry in the diffuse scattering is associated with small crystallites that are highly distorted by the internal stresses.[5]

In addition to the effect of volume swelling, the amorphous regions also cause distortion of the structure in the form of shear waves which can be seen in Fig. 3. This effect can be seen in the scattering profiles calculated along the transverse direction along the (440) reflection, which are shown in Fig. 6. Note that the profiles shown in Fig. 6 are calculated with the shift to the new position of the Bragg peak which moves from (440) (off-central cut) to $(4-\xi,4-\xi,0)$ (central cut) as the volume increases. This allows us to see considerable diffuse scattering in the off-central cut, which is less clear in the central cut of this reflection. At a higher value $f_a=0.2$ only a broad peak remains at the position of the Bragg peak and the diffuse scattering parts of the scattered intensity broaden.

In order to compare the effects of swelling and shearing the transverse component of the scattering profile needs to be calculated along the central cut of a particular reflection to ensure that both transverse and longitudinal components are on the same scale of intensity. In Fig. 7 we show scattering profiles for (800) reflection calculated along the longitudinal and transverse component. The latter profile is calculated at values of q which correspond to the new position of the Bragg peak $(8-\xi,0,0)$, $\xi=0.35$. The intensity of the Bragg peak in this reflection is weaker than the previous reflection which enables one to see considerable diffuse scattering in the central cut of the transverse component. As can be seen from the comparison of diffuse scattering of transverse and longitudinal components in Fig. 7, the degree of shearing is comparable with swelling in our model. Such a considerable shearing is consistent with the one observed recently in the diffuse scattering profiles of radiation-damaged zircon.[8]

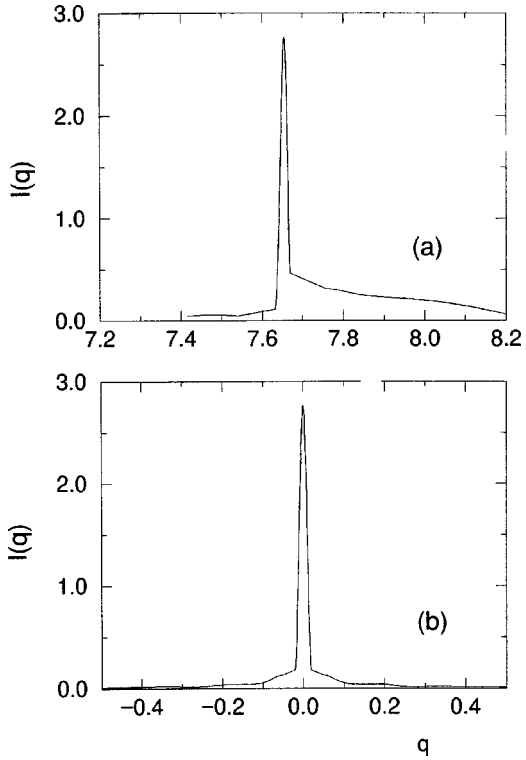

FIG. 7. Dependence of intensity $I(q)$ on q for (800) reflection at $f_a=0.40$ for (a) longitudinal direction and (b) transverse direction.

We tried to establish whether the existence of percolation points has an effect on the behavior of the scattering profiles. Once the second percolation point is reached and the percolating crystalline cluster is broken into disconnected ''floating'' crystalline regions these regions start rotating and shifting relative to each other, which could significantly reduce their coherence in contributing to the scattered intensity. However, there is no clear change of scattering profiles behavior at the values of dose corresponding to the second percolation point. The reason for this is the same as for the smooth behavior of the total volume swelling at the second percolation point: crystalline areas start distorting well before the percolation point is reached due to the local stresses imposed by adjacent swelled amorphous regions. This makes the scattering profiles insensitive to the percolation.

V. CONCLUSIONS

In summary, we have proposed a general model of the irradiated material which undergoes percolation-type transition from crystalline to amorphous state and have studied the effect of percolation on the bulk properties in the sample. Our model gives good reproduction of scattering profiles observed experimentally in zircon,[8] including the asymmetry of diffuse scattering and effects of swelling and shearing. Swelling of the undamaged crystalline parts naturally arises in this model which can be explained by interaction of those parts with adjacent swelled amorphous parts.

We also remark that in addition to bulk properties, the effect of percolation on transport properties in a sample may be of interest. If a particle is more likely to diffuse through the interface between crystalline and amorphous phase in a sample than through either of those phases, then an increase in diffusion can be observed in the $f1<f_a<f2$ regime, when both crystalline and amorphous percolating clusters exist. This has yet to be verified experimentally.

ACKNOWLEDGMENTS

The authors are grateful to EPSRC (Grant No. GR/L65888) for financial support and K.T. is grateful to the Cambridge Overseas Trust for support. The calculations were performed using the Hitachi computers of the High Performance Computing Facility in Cambridge. The authors are also grateful to Dr. Rios for helpful discussions.

[1] W. J. Weber, J. Am. Ceram. Soc. **76**, 1729 (1993).
[2] W. J. Weber, R. C. Ewing, and L. M. Wang, J. Mater. Res. **9**, 688 (1993).
[3] J. F. Gibbons, Proc. IEEE **60**, 1602 (1972).
[4] S. Rios, E. K. H. Salje, M. Zhang, and R. C. Ewing, J. Phys.: Condens. Matter **12**, 2401 (2000).
[5] E. K. H. Salje, J. Chrosch, and R. C. Ewing, Am. Mineral. **84**, 7 (1999).
[6] D. Stauffer and A. Aharony, *Introduction to Percolation Theory*, 2nd ed. (Taylor and Francis, London, 1992).
[7] W. Smith and T. Forester, J. Mol. Graphics **14**, 136 (1996).
[8] S. Rios and E. K. H. Salje, J. Phys.: Condens. Matter **11**, 8947 (1999).
[9] H. Holland and D. Gottfried, Acta Crystallogr. **8**, 291 (1955).
[10] T. Murakami, B. Chakoumakos, R. Ewing, G. Lumpkin, and W. Weber, Am. Mineral. **76**, 1510 (1991).